

## Nonclassical thermal effects in Stokes' second problem

P. Puri and P. K. Kythe, New Orleans, Louisiana

(Received February 4, 1992; revised April 6, 1994)

**Summary.** The MCF model is used to study the nonclassical heat conduction effects in Stokes' second problem. The structure of the waves and the influence of the thermal relaxation time on the temperature and velocity fields are investigated. The displacement thickness, skin friction and the rate of the heat transfer at the plate are determined.

### 1 Introduction

In classical unsteady heat transfer problems, the basic equations are derived from Fourier's law of heat conduction, which results in a parabolic equation for the temperature field and an infinite speed of heat propagation, thus violating the principle of causality. Ackerman et al. [1] established the second sound in solid helium, which gave a finite speed of propagation of thermal waves. Chester [2], Kaliski [3], Lord and Shulman [4], Green and Lindsay [5], and others have developed equations of thermoelasticity, which permit finite speed of thermoelastic propagation. However, there has been very little corresponding development in fluid dynamics. Lindsay and Straughan [6] studied acceleration waves and second sound in a perfect fluid. McTaggart and Lindsay [7] used a non-Fourier heat flux law and analyzed the effect of modified heat conduction equations in the Bénard problem. A detailed history of the development of nonclassical generalizations of Fourier's law is given in Joseph and Preziosi [8]. They state that the Cattaneo equation is the most obvious and simple generalization of Fourier's law that gives rise to finite speeds of propagation.

McTaggart and Lindsay [7] have shown that there is a major difference in the results of the Bénard problem when nonclassical effects are taken into account. This is due to the "major role played by the time constant of the Maxwell-Cattaneo theory". It is, therefore, of some interest to investigate the nonclassical heat conduction effects on simple unsteady flows.

In this article we propose to study a simple unsteady flow problem which deals with the nonclassical heat conduction effects and structure of waves in Stokes' second problem which may be of some significance in astrophysical applications. We have used the so-called MCF (Maxwell-Cattaneo-Fox) model as developed in McTaggart and Lindsay [7]. In this model the nonclassical constitutive equation for the heat-flux vector  $\mathbf{q}$  is given by the Maxwell-Cattaneo equation

$$\tau(\dot{q}_i - \omega_{ij}q_j) = -q_i - \kappa\theta_{,i}, \quad (1)$$

where  $\omega_{ij}$  is the vorticity,  $\kappa$  the thermal conductivity,  $\theta$  the temperature, and  $\tau$  the thermal relaxation time. If  $\omega_{ij} = 0$ , Eq. (1) reduces to that of the Cattaneo model, and for  $\tau = 0$  it becomes Fourier's law (see Joseph and Preziosi [8]). While there are other good models to choose from,

the Cattaneo law, as stated in Joseph and Preziosi [8], has many desirable properties, e.g., the steady heat flow may be induced by temperature gradients and gives rise to finite speeds of propagation.

The dimensionless thermal relaxation time, defined as  $\lambda = CP$ , where  $C$  and  $P$  are the Cattaneo and the Prandtl numbers respectively, exhibits a definite influence on the structure of the waves. It significantly modifies their behavior. The number  $\lambda$  also appears in generalized thermoelasticity (see Puri [9] where it is defined as  $m$ ) and is shown to be of order  $10^{-2}$ . Again as noted in McTaggart and Lindsay [7], the Cattaneo number  $C$  may not be very small in astrophysical applications. For example,  $C$  is of order  $10^{-2}$  in a low temperature hydrogen gas. Hence, a qualitative and quantitative analysis of the wave structure is desirable. However, the thermal relaxation time  $\lambda$  does not appreciably change the magnitude of the temperature and velocity fields.

The waves produced by the oscillations of the plate or of temperature imposed on the plate exhibit the following structure: There exists a progressive dispersive thermal wave-train in the temperature field with a velocity which approaches the velocity of similar waves in the classical case. In the velocity field, there exist two types of dispersive progressive wave-trains, one of which represents the classical Stokes waves except for a phase lag, while the other is similar to the above thermal wave-train except for the amplitude and phase lag.

## 2 Mathematical analysis

We will consider Stokes' second problem (see, e.g., Schlichting [10]). Let a viscous incompressible fluid rest adjacent to a vertical flat plane in the  $xy$ -plane and occupy the space  $z > 0$ , with  $x$ -axis in the vertical direction. The flow is induced by oscillation of the plate, or by its periodic heating, or both. The plate initially at rest and at constant temperature  $\theta_\infty$  which is the free stream temperature is moved with a velocity  $U_0 e^{i\omega t}$  in its own plane along the  $x$ -axis, and its temperature is subjected to a periodic heating of the form  $(\theta_w - \theta_\infty) e^{i\omega t}$ , where  $\theta_w (\neq \theta_\infty)$  is some constant.

The basic equations of continuity, momentum, and energy, governing such a flow, subject to the Boussinesq approximation, are

$$v_{i,i} = 0, \quad (2)$$

$$\rho \dot{v}_i = -p_{,i} + \mu \nabla^2 v_i - \rho [1 - \alpha(\theta - \theta_\infty)] g \delta_{i1} + t_{ki,k}, \quad (3)$$

$$\rho \dot{\varepsilon} = -q_{i,i} + t_{ik} d_{ik} \quad (4)$$

where the vector  $\mathbf{v} = (u, 0, 0)$  represents the velocity,  $\rho$  the density,  $\mu$  the dynamic viscosity,  $p$  the pressure,  $\varepsilon$  the specific internal energy,  $\alpha$  the coefficient of thermal expansion,  $g$  the acceleration due to gravity,  $t_{ik}$  the non-Newtonian stress tensor, and  $d_{ik}$  the strain tensor. Taking into account the geometry of the problem which results in the disappearance of the dissipative terms and noting that  $t_{ik} \equiv 0$  for the MCF model (see McTaggart and Lindsay [7]), Eqs. (2)–(3) reduce to the following equation of motion:

$$u_t = \nu u_{zz} + g\alpha(\theta - \theta_\infty). \quad (5)$$

Equation (1), after substitution into (4), gives

$$\rho c_p \dot{\theta} = -q_{i,i}, \quad (6)$$

since  $\varepsilon = c_p \theta$  for the MCF model. If we drop the nonlinear terms  $\tau \omega_{ij} q_j$  in (1) because  $\tau$  and  $\omega$  are small quantities, we get

$$\tau \dot{q}_{i,i} = -q_{i,i} - \kappa \theta_{,ii}. \quad (7)$$

Eliminating  $q_{i,i}$  between (6) and (7) we find that

$$-\rho c_p \tau \ddot{\theta} = \rho c_p \dot{\theta} - \kappa \theta_{,ii},$$

which in one-dimensional form, after dropping the convective terms (because these terms become automatically zero), leads to

$$\tau \theta_{tt} + \theta_t = \frac{\kappa}{\rho c_p} \theta_{zz}. \quad (8)$$

Note that the term  $\tau \theta_{tt}$  in (8) is necessary to ensure finite speed of propagation. We shall use the nondimensional quantities

$$z = \frac{v}{U_0} z', \quad u = U_0 u', \quad t = \frac{v}{U_0^2} t', \quad \frac{\theta - \theta_\infty}{\theta_w - \theta_\infty} = \theta',$$

$$G = \frac{v g \alpha (\theta_w - \theta_\infty)}{U_0^3}, \quad P = \frac{v \rho c_p}{\kappa}, \quad C = \frac{\tau \kappa U_0^2}{v^2 \rho c_p}, \quad \lambda = \frac{\tau U_0^2}{v} = CP, \quad (9)$$

where  $G$  is the Grashof number. Then the governing equations (5) and (8) for the flow and heat conduction, after suppressing the primes, become

$$u_t = u_{zz} + G\theta, \quad (10)$$

$$\lambda P \theta_{tt} + P \theta_t = \theta_{zz}. \quad (11)$$

The boundary conditions are

$$u(0, t) = e^{i\omega t} = \theta(0, t), \quad u(\infty, t) = 0 = \theta(\infty, t). \quad (12)$$

Taking  $u(z, t) = U(z) e^{i\omega t}$ , and  $\theta(z, t) = \Theta(z) e^{i\omega t}$ , Eqs. (10), (11), and the boundary conditions (12) yield

$$U'' - i\omega U = -G\Theta, \quad (13)$$

$$\Theta'' + (\lambda P \omega^2 - i\omega P) \Theta = 0, \quad (14)$$

$$U(0) = \Theta(0) = 1, \quad U(\infty) = \Theta(\infty) = 0. \quad (15)$$

The solutions of (13)–(15) are

$$U(z) = e^{-mz} - (G_1 + iG_2) \{e^{-mz} - e^{-z(r_1 + ir_2)}\}, \quad (16)$$

$$\Theta(z) = e^{-z(r_1 + ir_2)}, \quad (17)$$

where

$$m = (1 + i) \sqrt{\omega/2}, \quad r_{1,2} = \sqrt{\omega P \frac{(\sqrt{1 + \lambda^2 \omega^2} \mp \lambda \omega)}{2}}, \quad (18)$$

$$G_1 + iG_2 = \frac{G[\lambda P \omega^2 - i\omega(1 - P)]}{\lambda^2 P^2 \omega^4 + \omega^2(1 - P)^2}. \quad (19)$$

From (16), we find that

$$\begin{aligned} \operatorname{Re} u(z, t) = & e^{-z\sqrt{\omega/2}} \cos(\omega t - z\sqrt{\omega/2}) - e^{-z\sqrt{\omega/2}} [G_1 \cos(\omega t - z\sqrt{\omega/2}) \\ & - G_2 \sin(\omega t - z\sqrt{\omega/2})] + e^{-r_1 z} [G_1 \cos(\omega t - r_2 z) - G_2 \sin(\omega t - r_2 z)]. \end{aligned} \quad (20)$$

In the classical case, the solutions for both temperature and velocity fields can be obtained by taking  $\lambda = 0$  in (17) and (20) respectively. Then

$$\Theta(z) = e^{-(1+i)z\sqrt{\omega P/2} + i\omega t} \quad (21)$$

and  $G_1 = 0$ , and  $G_2 = 1/\omega(P - 1)$ . Thus  $P = 1$  becomes a singular case, and the solution for the velocity field in the classical case for  $P = 1$  has to be obtained directly, which is given by

$$u = \left( 1 + \frac{(1-i)Gz}{2\sqrt{2\omega}} \right) e^{i\omega t - (1+i)z\sqrt{\omega/2}}. \quad (22)$$

The standard definition of displacement thickness  $\delta^*$  is

$$\delta^* = \int_0^{\infty} \left( 1 - \frac{u}{U_f} \right) dz, \quad (23)$$

where  $U_f$  is the free stream velocity. In our case, the plate is moving while the free stream is stationary. Therefore, the formula (23) is modified, in the nondimensional form, as

$$\delta^* = \int_0^{\infty} u dz. \quad (24)$$

This formula can also be obtained by imparting to the entire system a negative velocity equal to the velocity of the plate. Using the formula (24) the absolute value of the displacement thickness is given by

$$|\delta^*| = \left| \frac{1}{m} - (G_1 + iG_2) \left( \frac{1}{m} - \frac{1}{(r_1 + ir_2)} \right) \right| \quad \text{for all } P, \quad \lambda \neq 0. \quad (25)$$

This thickness, in the classical case, is  $|\delta^*| = |1/m|$  in the absence of heat transfer. But in the singular case  $P = 1$  and  $\lambda = 0$ , it is given by

$$|\delta^*| = \frac{1}{\sqrt{\omega}} \sqrt{1 + G^2/4\omega^2}. \quad (26)$$

The skin friction on the plate is proportional to

$$\begin{aligned} \operatorname{Re} \frac{\partial u}{\partial z} \Big|_{z=0} = & \cos \omega t \{ G_2(r_2 - \sqrt{\omega/2}) - G_1(r_1 - \sqrt{\omega/2}) - \sqrt{\omega/2} \} \\ & + \sin \omega t \{ G_1(r_2 - \sqrt{\omega/2}) + G_2(r_1 - \sqrt{\omega/2}) - \sqrt{\omega/2} \}. \end{aligned} \quad (27)$$

The rate of heat transfer at the plate is given by

$$-\kappa \frac{\partial \theta}{\partial z} \Big|_{z=0} = \kappa(r_1 \cos \omega t - r_2 \sin \omega t). \quad (28)$$

### 3 Discussion

The oscillatory nature of the flow generates waves in both temperature and velocity fields. Although these waves decay rapidly, it is of some interest to understand their structure.

#### *Wave structure of thermal waves*

The solution (17) exhibits a progressive dispersive wave-train with a wave-front at  $z = \omega t/r_2$ , wave number  $r_2$ , velocity  $\omega/r_2$ , attenuation coefficient  $r_1$ , and group velocity

$$\frac{2\sqrt{2\omega(1 + \lambda^2\omega^2)}}{\sqrt{P}(\lambda\omega + \sqrt{1 + \lambda^2\omega^2})^{3/2}}, \quad (29)$$

which approaches  $2\sqrt{2\omega/P}$  as  $\lambda \rightarrow 0$ . This velocity is the same as in the classical case ( $\lambda = 0$ ). The depth of penetration of this wave is  $2\pi/r_2$ . In the case when  $\omega$  is small, we find that  $r_1 = r_2 \approx \sqrt{P\omega/2}$ . But if the product  $\lambda\omega$  is large, we find that  $r_1 \approx \frac{\sqrt{P/\omega}}{2\lambda}$ ,  $r_2 \approx \omega\sqrt{\lambda P}$ . In this case, then, the wave velocity is  $1/\sqrt{\lambda P}$ . Since  $\lambda$  is very small, the speed of the thermal wave is huge, and this wave decays very fast.

#### *Wave structure of velocity field*

The solution (16) exhibits two types of dispersive progressive wave-trains: One has a wave-front at  $z = t\sqrt{2\omega}$ , which corresponds to the classical Stokes waves. The difference between the classical and the present case is that a layer at a distance  $z$  from the plate oscillates with a phase lag of  $z\sqrt{\omega/2} - \psi_1$ , where

$$\tan \psi_1 = \frac{\omega(P-1)}{\lambda^2 P^2 \omega^4 + \omega^2(P-1)^2 - G\lambda P \omega^2}. \quad (30)$$

For  $P = 1$ , this reduces to the classical case ( $\psi_1 = 0$ ). The other wave-train is similar to the above mentioned thermal wave, except for the amplitude and the phase lag which is equal to  $zr_2 - \psi_2$ , where

$$\tan \psi_2 = \frac{P-1}{G\lambda P \omega}. \quad (31)$$

In this case we note that  $\psi_2 = 0$  for  $P = 1$ . From (22) we find that for  $P = 1$  in the classical case of the velocity field, the above two wave-trains coalesce into one with a wave-front at  $z = t\sqrt{2\omega}$ , and a phase lag of  $(z/\sqrt{2} - \phi)/\omega$  for a fluid layer at a distance  $z$  from the plate, where

$$\tan \phi = -\frac{Gz}{Gz + 2\sqrt{2\omega}}. \quad (32)$$

#### *Temperature field*

The effect of  $\lambda$  on  $\theta$  is not appreciable for small frequencies. However, for large  $\omega$  the presence of  $\lambda$  affects both  $|\theta|$  and  $\text{Re } \theta$ . As can be seen from Figs. 1 and 2, the magnitude  $|\theta|$  reduces as  $\lambda$

increases for both small and large  $P$ ; moreover, an increase in  $\lambda$  decreases the thermal boundary layer.

A similar delay response time is also observed in  $\text{Re } \theta$  as seen in Fig. 3.

### Velocity field

The influence of  $\lambda$  on both  $\text{Re } u$  and  $|u|$  is found to be very small, although it changes the character of the velocity field. Since  $\lambda$  takes very small values, we have presented the graphs of  $\text{Re } u$  and  $|u|$  in Figs. 4 and 5 for  $\lambda = 0.005$ ,  $\omega = 10$ ,  $G = \pm 5$  and  $t = 0.1$ . For large  $\omega$ , the influence of both  $\lambda$  and  $G$  is negligible; we have sketched both  $\text{Re } u$  and  $|u|$  in Figs. 6 and 7 for  $\lambda = 0.005$ ,  $\omega = 1000$ ,  $G = -5$ . As can be seen from Fig. 5, an increase in  $G$  increases the fluid boundary layer. The thermal boundary layer is much smaller than the fluid boundary layer.

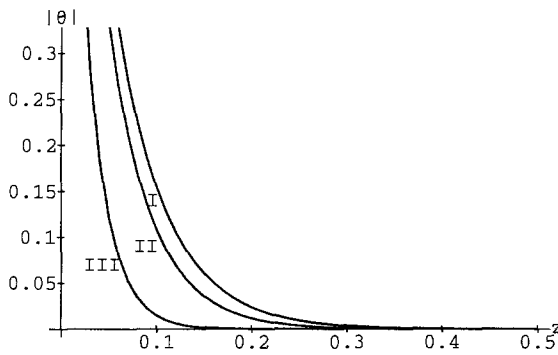


**Fig. 1.** Behavior of  $|\theta|$  vs.  $z$  for  $\omega = 1000$ ,  $P = 0.7$ ,  $\lambda = 0$  (I),  $\lambda = 0.001$  (II), and  $\lambda = 0.005$  (III)

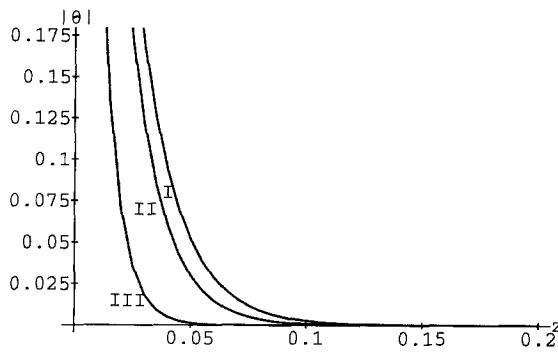


**Fig. 2.** Behavior of  $|\theta|$  vs.  $z$  for  $\omega = 1000$ ,  $P = 7.0$ ,  $\lambda = 0$  (I),  $\lambda = 0.001$  (II), and  $\lambda = 0.005$  (III)

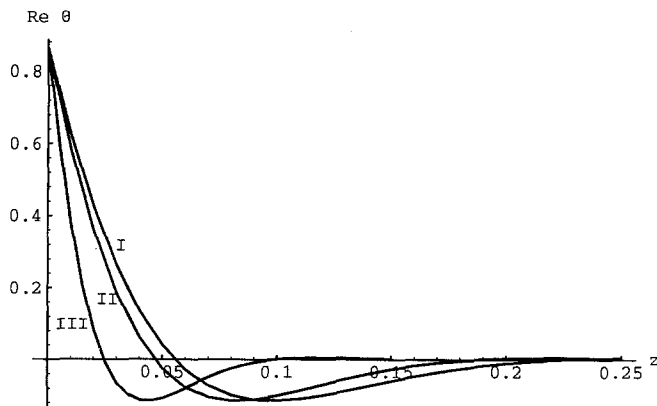


**Fig. 3.** Behavior of  $\text{Re } \theta$  vs.  $z$  for  $\omega = 1000$ ,  $P = 0.7$ ,  $\lambda = 0$  (I),  $\lambda = 0.001$  (II), and  $\lambda = 0.005$  (III) at  $t = 0.1$

The velocity field can be regarded as consisting of two layers: one corresponding to  $e^{-mz}$  and the other to  $e^{-(r_1+ir_2)z}$ . The former is the Stokes-Rayleigh layer which is of order  $O(1/\sqrt{\omega})$ , while the latter is the thermal layer which is of order  $O(1/r_1)$ .

In order to observe the effect of  $\lambda$  on  $\text{Re } u$  we have presented some data in Tables 1 and 2 below. Thus, in Table 1, which is for  $G = -5$ , it can be seen that an increase in  $\lambda$  tends to decrease  $\text{Re } u$  up to  $z = 0.26$  for an increase in  $\lambda$  from 0.0 to 0.005, and increase it thereafter; again,  $\lambda$  increases  $\text{Re } u$  up to  $z = 0.22$  for an increase in  $\lambda$  from 0.005 to 0.01, and decreases it

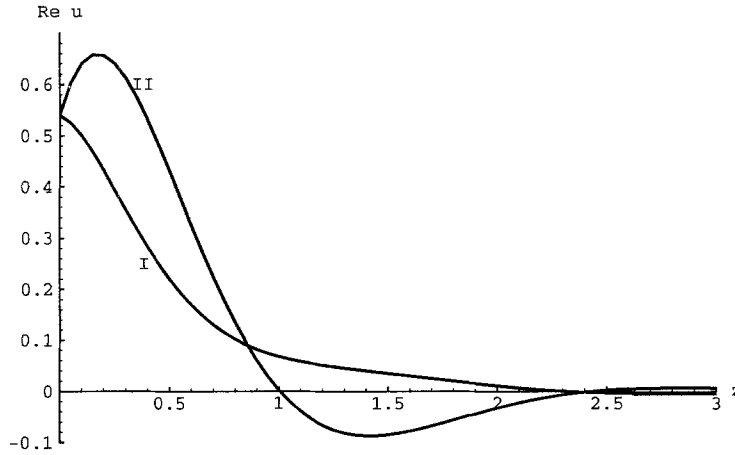


**Fig. 4.** Behavior of  $\text{Re } u$  vs.  $z$  for  $\omega = 10$ ,  $P = 0.7$ ,  $\lambda = 0.005$ ,  $G = -5$  (I), and  $G = 5$  (II) at  $t = 0.1$

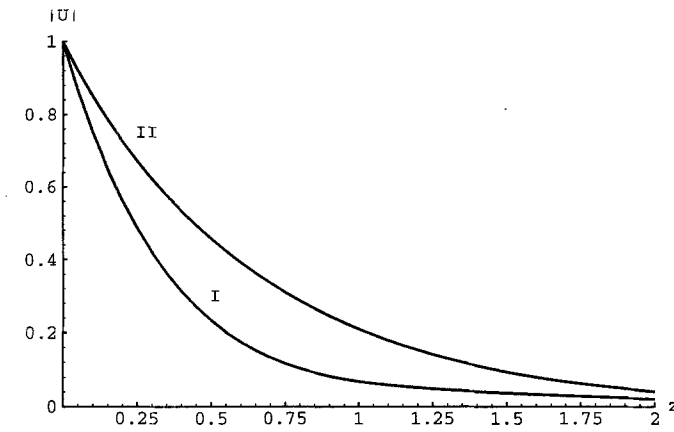


**Fig. 5.** Behavior of  $|u|$  vs.  $z$  for  $\omega = 10$ ,  $P = 0.7$ ,  $\lambda = 0.005$ ,  $G = -5$  (I), and  $G = 5$  (II) at  $t = 0.1$

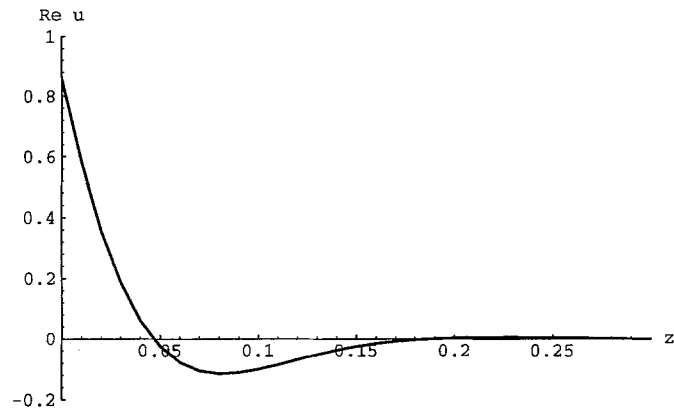


**Fig. 6.** Behavior of  $\text{Re } u$  vs.  $z$  for  $\omega = 1000$ ,  $P = 0.7$ ,  $G = -5$ , and  $\lambda = 0.005$  at  $t = 0.1$

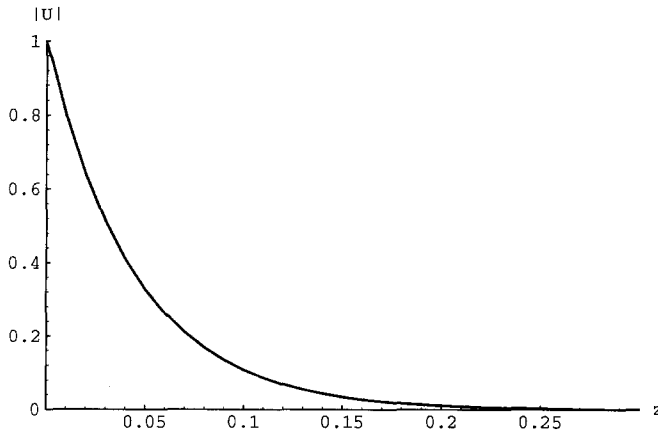


**Fig. 7.** Behavior of  $|u|$  vs.  $z$  for  $\omega = 1000$ ,  $P = 0.7$ ,  $G = -5$ , and  $\lambda = 0.005$  at  $t = 0.1$

**Table 1.**  $\text{Re } u$  at  $t = 0.1$ ,  $\omega = 10$ ,  $P = 0.7$ , and  $G = -5$

$\lambda$	$z = 0$	$z = 0.2$	$z = 0.21$	$z = 0.22$	$z = 0.26$	$z = 0.27$	$z = 0.3$
0.0	0.540302	0.43217	0.424626	0.417018	0.386215	0.378483	0.355388
0.005	0.540302	0.432036	0.424508	0.416917	0.386211	<u>0.378511</u>	0.355524
0.01	0.540302	0.431996	0.424487	<u>0.416919</u>	0.386329	0.378664	0.3558

**Table 2.**  $\text{Re } u$  at  $t = 0.1$ ,  $\omega = 10$ ,  $P = 0.7$ , and  $G = 5$

$\lambda$	$z = 0$	$z = 0.2$	$z = 0.21$	$z = 0.22$	$z = 0.26$	$z = 0.27$	$z = 0.3$
0.0	0.540302	0.656184	0.654077	0.6514	0.635479	0.630307	0.612286
0.005	0.540302	0.656318	0.654195	0.651501	0.635482	<u>0.63028</u>	0.61215
0.01	0.540302	0.656358	0.654216	<u>0.6515</u>	0.635365	0.630127	0.611874

thereafter. This behavior is reversed for  $G = 5$ , as is obvious from Table 2. The underlined data are the critical values of  $\text{Re } u$  with respect to  $\lambda$ ; at these values there is a reversal in response to an increase in  $\lambda$ .

A comparison of Figs. 4 (I) and 6, and Figs. 5 (I) and 7 shows that an increase in  $\omega$  tends to increase the decay in the velocity  $\text{Re } u(z, t)$ . This is also obvious from expression (20).

## 4 Conclusions

The presence of  $\lambda$  modifies the purely thermal wave. In particular, the classical wave velocity  $\sqrt{2\omega/P}$  modifies to  $\omega/r_2$  in the nonclassical case and approaches a finite value of  $1/\sqrt{\lambda P}$  for large  $\omega$ . This is a major but expected deviation from the classical case.

Although  $\lambda$  modifies both temperature and velocity fields, this influence is, however, not uniform. It tends to increase the amplitude of both of these fields under some cases and to decrease it under other cases.

The solution for the velocity field exhibits two types of wave motion, one of which corresponds to the thermal wave and the other to the classical Stokes wave. The equation of motion is modified only to the extent that the temperature is modified.



## Acknowledgement

The authors thank the referees for some valuable comments and suggestions.

## References

- [1] Ackerman, C. C., Bertman, B., Fairbank, H. A., Guyer, R. A.: Second sound in solid helium. *Phys. Rev. Lett.* **16**, 789–791 (1966).
- [2] Chester, M.: Second sound in solids. *Phys. Rev.* **131**, 2013–2015 (1963).
- [3] Kaliski, S.: Wave equations in thermoelasticity. *Bull. Acad. Polon. Sci. Ser. Sci. Tech.* **13**, 253–260 (1965).
- [4] Lord, H. W., Shulman, Y.: A generalized dynamical theory of thermoelasticity. *J. Mech. Phys. Solids* **15**, 299–309 (1967).
- [5] Green, A. E., Lindsay, K. A.: Thermoelasticity. *J. Elasticity* **2**, 1–7 (1972).
- [6] Lindsay, K. A., Straughan, B.: Acceleration waves and second sound in a perfect fluid. *Arch. Rat. Mech. Anal.* **68**, 53–87 (1978).
- [7] McTaggart, C. L., Lindsay, K. A.: Nonclassical effects in the Bénard problem. *SIAM J. Appl. Math.* **45**, 70–92 (1985).
- [8] Joseph, D. D., Preziosi, L.: Heat waves. *Rev. Modern Phys.* **61**, 41–73 (1989).
- [9] Puri, P.: Plane waves in generalized thermoelasticity. *Int. J. Eng. Sci.* **11**, 735–744 (1973); **13**, 339–340 (1975).
- [10] Schlichting, H.: *Boundary layer theory*, 4th ed., p. 75. New York: McGraw-Hill 1960.

**Authors' address:** P. Puri and P. K. Kythe, Department of Mathematics, University of New Orleans, New Orleans, LA 70148, U.S.A.